Electrostatic Interaction between Retinylidene Chromophore and Opsin in Rhodopsin Studied by Fluorinated Rhodopsin Analogues†

Yoshinori Shichida,‡ Toshirou Ono,‡ Tôru Yoshizawa,*,‡ Hiroyuki Matsumoto,§,∥ Alfred E. Asato,§ Jesmael P. Zingoni,§ and Robert S. H. Liu§

Department of Biophysics, Faculty of Science, Kyoto University, Kyoto 606, Japan, and Department of Chemistry, University of Hawaii, Honolulu, Hawaii 96844

Received January 13, 1987; Revised Manuscript Received March 6, 1987

ABSTRACT: Photochemical reactions of fluorinated rhodopsin analogues (F-rhodopsins) prepared from 10- or 12-fluorinated retinals (10- or 12-F-retinals) and cattle opsin were investigated by means of low-temperature spectrophotometry. On irradiation with blue light at liquid nitrogen temperature (−191 °C), the F-rhodopsins were converted to their respective batho intermediates. On warming, they decomposed to their respective fluororetinals and cattle opsin through lumi and meta intermediates. There was a difference in photochemical behavior between batho-12-F-rhodopsin and batho-10-F-rhodopsin. Upon irradiation with red light at −191 °C, batho-12-F-rhodopsin was converted to a mixture of 12-F-rhodopsin and 9-*cis*-12-F-rhodopsin like that of the natural bathorhodopsin, whereas batho-10-F-rhodopsin was not converted to 9-*cis*-10-F-rhodopsin but only to 10-F-rhodopsin. This fact suggests that the fluorine substituent at the C_{10} position (i.e., 10-fluoro) of the retinylidene chromophore may interact with the protein moiety during the process of isomerization of the chromophore or in the state of the batho intermediate. On irradiation with blue light at −191 °C, 9-*cis*-10-F-rhodopsin was converted to another bathochromic intermediate that was different in absorption spectrum from batho-10-F-rhodopsin. 9-*cis*-10-F-rhodopsin was practically "photoinsensitive" at liquid helium temperature (−265 °C), whereas 10-F-rhodopsin was converted to a photo-steady-state mixture of 10-F-rhodopsin and batho-10-F-rhodopsin. The specific interaction between the fluorine atom at the C_{10} position of the retinylidene chromophore and the opsin was discussed in terms of electrostatic interactions.

Rhodopsin has an 11-*cis* retinal as its chromophore that covalently binds to the ϵ-amino group of lysine residue in the opsin moiety through a protonated Schiff base linkage. On irradiation of rhodopsin at liquid nitrogen temperature, it undergoes the photochemical conversion to bathorhodopsin through the excited state of rhodopsin and photorhodopsin (Shichida et al., 1984). Since the chromophore of bathorhodopsin is in an 11-trans form of a protonated retinylidene Schiff base, the photoisomerization of the reintylidene chromophore from the 11-cis to the 11-trans form has been implicated as being responsible for this conversion [see recent reviews of Ottolenghi (1982) and Yoshizawa et al. (1984)].

The photochemical reaction of bathorhodopsin is uniquely regiospecific; the chromophore easily photoisomerizes to the 11-cis or 9-cis isomer but never to the 13-cis isomer (Maeda et al., 1978, 1979). Free *all-trans*-retinal in a nonpolar solvent, however, is selectively isomerized at the methylated double bonds with a preference for the 13,14 double bond (Liu et al., 1983). Such a regioselective isomerization directed by the opsin moiety is seen in all of the known visual pigment analogues.

There are at least two kinds of interaction between the chromophore and opsin in rhodopsin, i.e., electrostatic and steric interactions; those may lead to the regioselective isomerization of the chromophore. The presence of secondary electrostatic interaction has been implicated from the bathochromic shift of the absorption spectrum of the retinylidene Schiff base in rhodopsin. Honig et al. (1979a,b) suggested the existence of an additional negative charge other than the counterion of the protonated Schiff base near the C_{12} and C_{14} positions, although it was recently suggested that the second negative charge may correspond to the second oxygen of the carboxylate group of the counterion of the Schiff base (Liu et al., 1984; Birge et al., 1985; Kakitani et al., 1985). On the other hand, the steric interaction between the conjugated double bond system of the chromophore and the opsin has been suggested on the basis of circular dichroism (CD) studies of rhodopsin, its intermediates (Yoshizawa & Shichida, 1982), and rhodopsin analogues (Balogh-Nair & Nakanishi, 1982).

Since the fluorine atom is highly electronegative, its substitution for a hydrogen atom in the retinylidene chromophore can affect not only the electronic property of the chromophore but also the interaction of the chromophore with opsin, especially the polarized or charged amino acid residue(s) near the chromophore. Therefore, rhodopsin analogues with a fluorinated retinylidene chromophore may provide useful information concerning the role of the electrostatic interaction on the photoisomerization process of the retinylidene chromophore of rhodopsin.

We report here the photochemical reaction of fluorinated rhodopsin analogues, i.e., 10-F- and 12-F-rhodopsins. The former exhibited a photoisomerization process that was uniquely regiospecific, indicating a specific chromophore–protein interaction between the C_{10} fluorine and opsin.

Materials and Methods

Synthesis and Purification of Fluororetinals. Both 10-F- and 12-F-retinals were synthesized by methods described previously (Matsumoto et al., 1980). The 9-cis and 11-cis isomers of these fluorinated retinals were isolated from their

† Work at Kyoto University was supported in part by Grants in Aid for Cooperative Research to T.Y. (60304098) and for Encouragement of Young Scientist to Y.S. (61780316) from the Japanese Ministry of Education, Science and Culture and by the Naito Foundation to Y.S. Work at the University of Hawaii was supported by a grant from the U.S. Public Health Service to R.S.H.L. (AM 17806).

* Author to whom correspondence should be addressed.

‡ Kyoto University.

§ University of Hawaii.

∥ Present address: Department of Biochemistry and Molecular Biology, College of Medicine, University of Oklahoma Health Science Center, Oklahoma City, OK 73190.

0006-2960/87/0426-4422$01.50/0

isomeric mixtures produced from all-trans forms by UV irradiation by means of preparative high-performance liquid chromatography (HPLC) (Altex $^1/_2$ in. × 1 ft 5 in. Lichrosorb column; solvent, 10% or 5% ether in hexane) and then stored at −80 °C until use.

Preparation of Rhodopsin Analogues. Cattle retinas were used as one of the starting materials for preparing fluorinated rhodopsin analogues. The rod outer segments (ROS) were isolated from the retinas by a conventional sucrose stepwise gradient method (Matsumoto et al., 1978) and then irradiated with orange light at wavelengths longer than 510 nm (>510 nm) in 10 mM HEPES[1] buffer containing 10 mM hydroxylamine (pH 7.0), for bleaching of rhodopsin in ROS to retinal oxime and opsin. To remove the unreacted hydroxylamine and retinal oxime, the ROS was washed 5 times with 10 mM HEPES buffer by centrifugation (10000*g*, 20 min) and treated with petroleum ether after lyophilization. Then, the ROS was suspended in 10 mM HEPES buffer (pH 7.0).

For preparing the F-rhodopsins, one of the retinal analogues in ethanol was added in the ROS suspension containing opsin and then incubated at 20 °C for about 12 h. After lyophilization, the dried ROS containing the rhodopsin analogue was washed with petroleum ether to remove unreacted retinal analogue.

The rhodopsin analogue was extracted from the ROS with 2% digitonin or 2% Ammonyx-LO. The sample extracted with 2% digitonin was stable against 10 mM hydroxylamine at 0 °C, while that extracted with 2% Ammonyx-LO was not. For low-temperature spectroscopy, the digitonin extract was mixed with glycerol and neutralized hydroxylamine in a final concentration of 66% or 75% and 10 mM, respectively, while the extract with 2% Ammonyx-LO was mixed with only glycerol after purification of the extract by column chromatography (hydroxylapatite–Celite system; Hong et al., 1982).

Spectrophotometry at Low Temperature. For measuring the absorption spectra at low temperature from 0 to −269 °C, specially designed glass cryostats with quartz windows (Yoshizawa, 1972; Yoshizawa & Shichida, 1982) were used. The temperature of the sample was monitored with a copper–constantan (above −196 °C) or a gold–chromel (above −269 °C) thermocouple attached to the sample cell holder. The sample was irradiated with light from a xenon lamp (2 kW, Ushio Co. Ltd.) which had passed through a glass cut-off filter (Toshiba Co. Ltd.) with or without an interference filter (Nihonshinku Co. Ltd.). Absorption spectra were measured with Hitachi 323 recording spectrophotometer. For correction of scattering of the sample, opal glasses were placed in both the sample and reference sides.

Results

Temperature Dependency of Absorption Spectra. At room temperature (20 °C), 12-F-rhodopsin has an absorption maximum at 506 nm that lies 8 nm longer in wavelength than that of cattle rhodopsin (498 nm) (Table I). On cooling from 20 to −191 °C, the absorption maximum of 12-F-rhodopsin shifted from 506 to 514 nm (Table I and Figure 1b). This bathocrhomic shift was very close to that in the case of cattle rhodopsin (from 498 to 505 nm).

10-F-rhodopsin (498 nm) was similar in absorption maximum to cattle rhodopsin at 20 °C and in the shape of the absorption spectrum to both cattle rhodopsin and 12-F-rhodopsin. On cooling to −191 °C, however, the absorption spectrum of 10-F-rhodopsin displayed two absorption peaks

[1] Abbreviation: HEPES, *N*-(2-hydroxyethyl)piperazine-*N*′-2-ethanesulfonic acid.

Table I: Absorption Spectral Properties of Original Pigments and Batho Intermediates in Rhodopsin and Fluorinated Rhodopsin Systems

pigment systems	absorption maximum (nm)[a] original	batho	relative extinction coeffi-cient[b]	bathochromic shift (cm^{-1})[c]
rhodopsin	505 (498)	543	1.1	1664
10-F-rhodopsin	495 (498)	562	1.6	2286
12-F-rhodopsin	514 (506)	572	1.1	2280

[a] Absorption maximum measured at −191 °C. The values in parentheses were measured at 20 °C. [b] Relative extinction coefficient at −191 °C (ratio of extinction coefficient of a batho intermediate to that of the original pigment). [c] Difference in wavenumber at absorption maximum between original pigment at 20 °C and its batho intermediate at −191 °C.

located at 495 and 530 nm, owing to vibronic structure (curve 1 in Figure 1c), which was never observed in rhodopsin and 12-F-rhodopsin (curves 1 of a and b in Figure 1, respectively). The appearance of the vibronic structure suggests that the chromophore of the 10-F-rhodopsin may be more planar or interact with opsin more rigidly than those of rhodopsin and 12-F-rhodopsin, consistent with the notion that the fluorine atom at the 10-position of the chromophore may form a specific interaction with an amino acid residue near the chromophore (see below).

Photochemical Reactions at −191 °C. Irradiation of rhodopsin as well as 9-*cis*-rhodopsin (isorhodopsin) with blue light at 437 nm (437-nm light) at liquid nitrogen temperature yielded a photo-steady-state mixture composed of rhodopsin, 9-*cis*-rhodopsin, and bathorhodopsin (Yoshizawa & Wald, 1963). Typical experimental results are shown in Figure 1a. The photochemical behavior of 12-F-rhodopsin at −191 °C (Figure 1b) is similar to that of rhodopsin (Liu et al., 1981). Namely, on irradiation of 12-F-rhodopsin with 437-nm light at −191 °C, the spectrum shifted to longer wavelengths with an isosbestic point at 532 nm during the early stage of the irradiation, owing to the formation of a bathoproduct (batho-12-F-rhodopsin). Prolonged irradiation yielded a photo-steady-state mixture composed of 12-F-rhodopsin, 9-*cis*-12-F-rhodopsin, and batho-12-F-rhodopsin. These components were readily interconvertible by light at −191 °C (Figure 1b, below). The same photo-steady-state mixture was produced when 9-*cis*-12-F-rhodopsin was used as a starting material. The spectra of 12-F-rhodopsin and batho-12-F-rhodopsin, however, were different in λ_{max} and extinction coefficient from those of cattle rhodopsin and its product (Table I).

On the other hand, 10-F-rhodopsin was different in photochemical behavior at 191 °C from rhodopsin and 12-F-rhodopsin (Figure 1c). Irradiation of 10-F-rhodopsin with 440-nm light led to a bathochromic shift of the spectrum with a clear isosbestic point at 504 nm until the photo-steady-state mixture (curve 10 in Figure 1c, above; curve 2 in Figure 1c, below) was produced. After reirradiation of the mixture with orange light (>590 nm), the spectrum (curve 2 in Figure 1c, below) showed a hypsochromic shift with formation of an isosbestic point at the same position (504 nm). A noteworthy point is that the final spectrum (curve 3 in Figure 1c, below) coincided with the original spectrum (curve 1 in Figure 2, below), indicating no formation of the 9-cis form of 10-F-rhodopsin (9-*cis*-10-F-rhodopsin) by irradiation of 10-F-rhodopsin and batho-10-F-rhodopsin at −191 °C. The presence of the sharp isosbestic point in both the forward and backward photochemical processes is additional evidence that the photo-steady-state mixture involves only two components. These results clearly demonstrate that batho-10-F-rhodopsin is

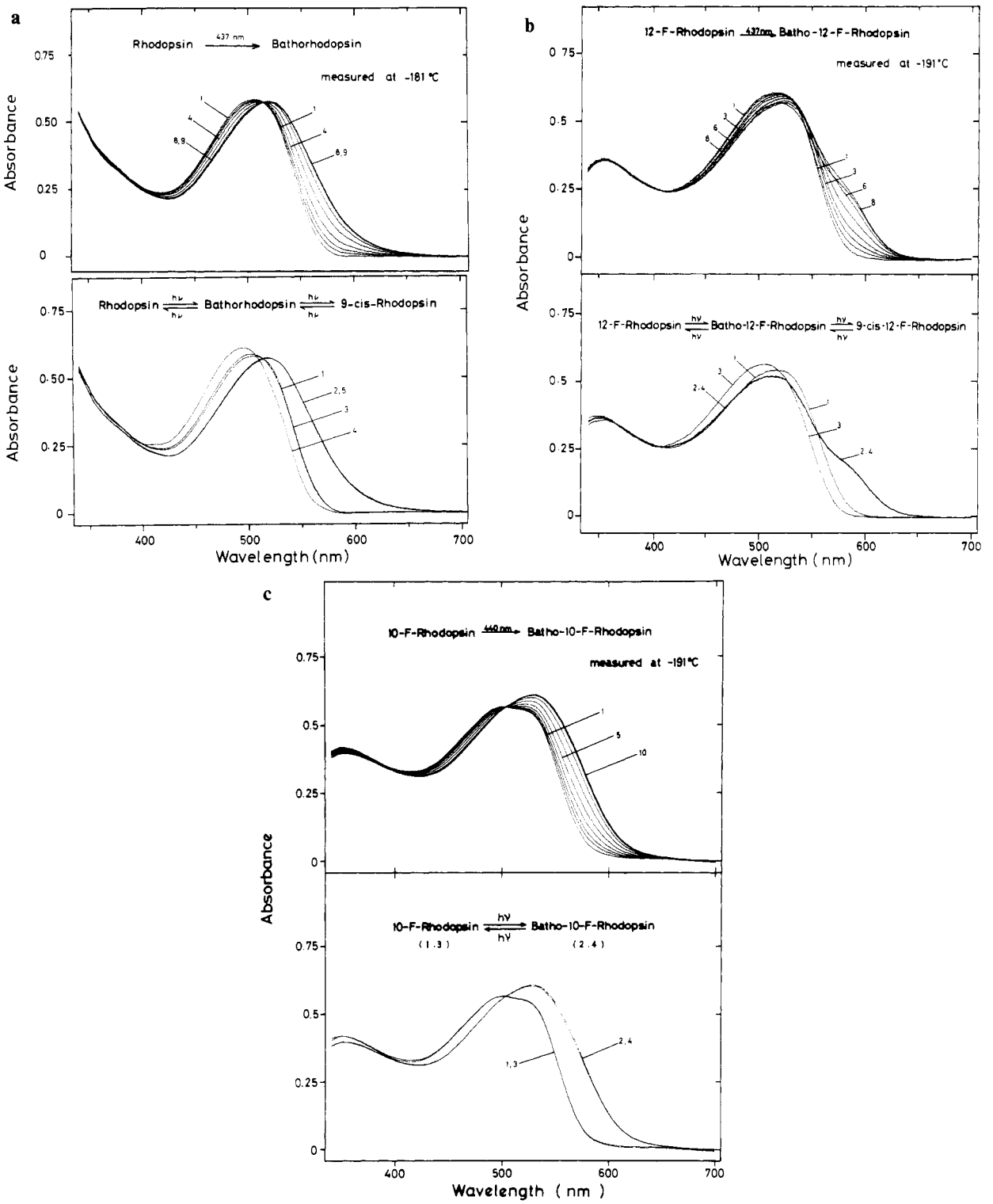

FIGURE 1: Photochemical reactions of cattle rhodopsin, 12-F-rhodopsin, and 10-F-rhodopsin at liquid nitrogen temperature. (a) Cattle rhodopsin. (Above) Course of conversion of cattle rhodopsin to bathorhodopsin. A rhodopsin–66% glycerol mixture (in 2% Ammonyx-LO dissolved in 10 mM HEPES buffer, pH 7.0; curve 1) was successively irradiated with 437-nm light at −181 °C for 5, 5, 10, 20, 40, 80, 160, and 320 s (curves 2-9). (Below) Photoreversibility among rhodopsin, 9-*cis*-rhodopsin, and bathorhodopsin at −181 °C. The rhodopsin–66% glycerol mixture (curve 1, identical with curve 1 above) was irradiated with 437-nm light at −181 °C for a total of 640 s (curve 2, identical with curve 9 above). The sample was then irradiated with red light (>630 nm) for 1256 s (curve 3). After futher irradiation with orange light (>570 nm) for 1200 s (curve 4), the sample was irradiated again with 437-nm light for 640 s (curve 5). (b) 12-F-rhodopsin. (Above) Course of conversion of 12-F-rhodopsin to batho-12-F-rhodopsin. A 12-F-rhodopsin–66% glycerol mixture (in 2% digitonin dissolved in 10 mM HEPES buffer, pH 7.0; curve 1) was successively irradiated with 437-nm light at −191 °C for 5, 5, 10, 20, 40, 80, and 160 s (curves 2–8). (Below) Photoreversibility among 12-F-rhodopsin, 9-*cis*-12-F-rhodopsin, and batho-12-F-rhodopsin. The 12-F-rhodopsin–66% glycerol mixture (curve 1, identical with curve 1 above) was irradiated with 437-nm light at −191 °C for 2560 s (curve 2). Then the sample was irradiated with red light (>610 nm) for 1280 s (curve 3). Finally, the sample was irradiated with 437-nm light again for 2560 s (curve 4). (c) 10-F-rhodopsin. (Above) Course of conversion of 10-F-rhodopsin to batho-10-F-rhodopsin. A 10-F-rhodopsin–66% glycerol mixture (in 2% digitonin dissolved in 10 mM HEPES buffer, pH 7.0; curve 1) was successively irradiated with 440-nm light at −191 °C for 5, 5, 10, 20, 40, 80, 160, 320, and 640 s (curves 2–10). (Below) Photoreversibility between 10-F-rhodopsin and batho-10-F-rhodopsin at −191 °C. The rhodopsin–66% glycerol mixture (curve 1, identical with curve 1 above) was irradiated with 440-nm light at −191 °C for 1280 s (curve 2, identical with curve 10 above). Then the sample was irradiated with orange light (>590 nm) for 1280 s (curve 3). Finally, the sample was irradiated with 440-nm light again for 1280 s (curve 4).

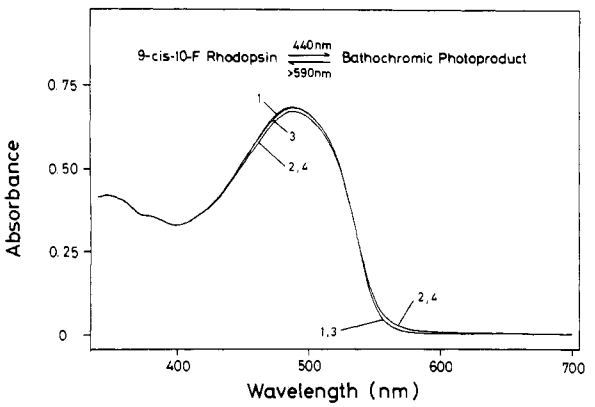

FIGURE 2: Photoreversibility between 9-*cis*-10-F-rhodopsin and its bathochromic intermediate at −191 °C. A 9-*cis*-10-F-rhodopsin–66% glycerol mixture (in 2% Ammonyx-LO dissolved in 10 mM HEPES buffer, pH 7.0; curve 1) was irradiated with 440-nm light at −191 °C for 1280 s (curve 2), then with orange light (>590 nm) for 1280 s (curve 3), and finally with 440-nm light again for 1280 s (curve 4).

converted by light only to 10-F-rhodopsin and not to 9-*cis*-10-F-rhodopsin.

The photochemical behavior of 9-*cis*-10-F-rhodopsin was also examined. Irradiation of 9-*cis*-10-F-rhodopsin with 440-nm light at −191 °C showed only a slight bathochromic shift (Figure 2). A bathochromic photoproduct in the photo-steady-state mixture was bleached to a mixture of presumably 10-F-retinal and opsin on warming to 20 °C. From the ratio of the absorbance at 486 nm of the sample after the warming to that of the original 9-*cis*-10-F-rhodopsin, the amount of the bathochromic photoproduct in the photo-steady-state mixture was estimated to be 5.9%. Although the isomeric form of the retinylidene chromophore of the bathochromic photoproduct is not identified yet, the results obtained clearly show that the photochemical product of 9-*cis*-10-F-rhodopsin is different from that of 10-F-rhodopsin. This anomalous photochemical behavior of 9-*cis*-10-F-rhodopsin was also observed at 20 and −265 °C. On exposure to yellow light at 20 °C, 9-*cis*-10-F-rhodopsin was found to be relatively insensitive (Liu et al., 1986). Only prolonged irradiation bleached it to an isomer of retinal oxime with a low extinction coefficient (approximately half of that of *all-trans*-retinal oxime). At −265 °C, 9-*cis*-10-F-rhodopsin was photoinsensitive, while 10-F-rhodopsin was converted to batho-10-F-rhodopsin without production of a hypso intermediate.

Absorption Spectra of Batho Intermediates. Absorption spectra of the original pigments and its batho intermediates in the native rhodopsin, 12-F-rhodopsin, and 10-F-rhodopsin systems were calculated by the usual method (Yoshizawa & Shichida, 1982), i.e., roughly speaking, by subtracting the spectra of original pigment and 9-cis-pigment in each system from the spectrum of the respective photo-steady-state mixture. As shown in Table I, batho-12-F-rhodopsin had an absorption maximum at 572 nm that was 58 nm longer in wavelength than that of 12-F-rhodopsin. The extinction coefficient of batho-12-F-rhodopsin was about 1.1 times larger than that of 12-F-rhodopsin. This ratio is in good agreement with that in the cattle rhodopsin system.

Batho-10-F-rhodopsin had an absorption maximum at 562 nm. Since the absorption spectrum of 10-F-rhodopsin at −191 °C had two peaks at 495 and 530 nm, the calculation of the difference in wavenumber at λ_{max} between 10-F-rhodopsin and bath-10-F-rhodopsin is not simple. Regarding that the difference in wavenumber at the absorption maximum between 10-F-rhodopsin at 20 °C and batho-10-F-rhodopsin (at −191 °C) approximate that between 10-F-rhodopsin at −191 °C and batho-10-F-rhodopsin, we obtained a value of 2286 cm^{-1}. This value was nearly equal to that of the 12-F-rhodopsin system (2280 cm^{-1}) and 1.37 times larger than that of the cattle rhodopsin system (1664 cm^{-1}) calculated under the same assumption.

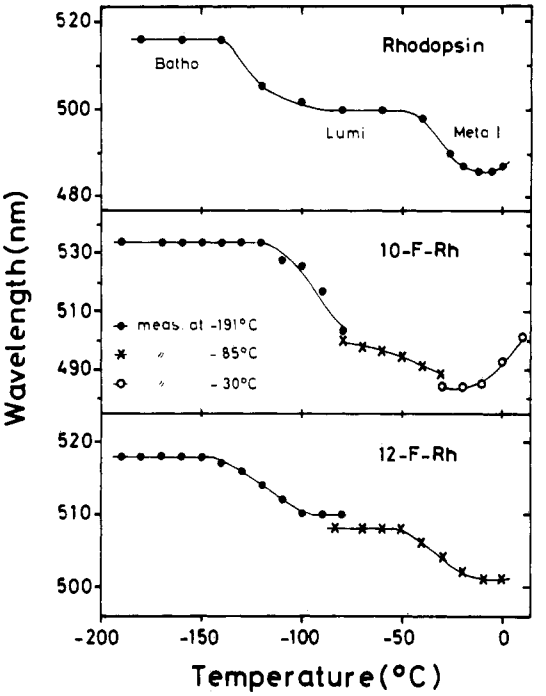

FIGURE 3: Changes in λ_{max} of the photo-steady-state mixtures of cattle rhodopsin (above), 10-F-rhodopsin (middle), and 12-F-rhodopsin (below) by stepwise warming. The sample was irradiated at −191 °C with blue light (rhodopsin and 12-F-rhodopsin, 437 nm; 10-F-rhodopsin, 440 nm) until a photo-steady-state mixture containing mainly batho intermediate was produced. Then it was warmed to a selected temperature (abscissa) and then recooled to −191 (●), −85 (×) or −30 °C (○) for measurement of the spectra.

It should be noted that the extinction coefficient of batho-10-F-rhodopsin is about 1.6 times bigger than that of 10-F-rhodopsin, larger than those of the rhodopsin (1.1) and 12-F-rhodopsin (1.1) systems.

In the 9-*cis*-10-F-rhodopsin system, the amount of bathochromic photoproduct in the photo-steady-state mixture was so small (5.9%) that it was difficult to accurately calculate the absorption spectrum. Rough estimation showed the absorption maximum of the photoproduct to be 520 ± 20 nm and its extinction coefficient to be about 0.63 times that of 9-*cis*-10-F-rhodopsin.

Intermediates in the Photobleaching Process. Figure 3 shows experimental results obtained by stepwise warming of each of the photo-steady-state mixtures of rhodopsin, 12-F-rhodopsin, and 10-F-rhodopsin from −191 to 0 °C, in which the minimum numbers of intermediates in the respective photobleaching processes were determined. Each of the photo-steady-state mixtures formed by irradiating the respective rhodopsins with blue light at −191 °C was warmed to a desired temperature and then recooled to −191, −85, or −30 °C for measurement of the spectrum. The wavelength at the maximum of each spectrum was plotted as a function of the temperature, to which the photo-steady-state mixture was warmed.

From the existence of plateau temperature ranges, three intermediates were detected in both 10-F- and 12-F-rhodopsin systems like the cattle rhodopsin system. The transition temperature of the intermediates of 12-F-rhodopsin was almost

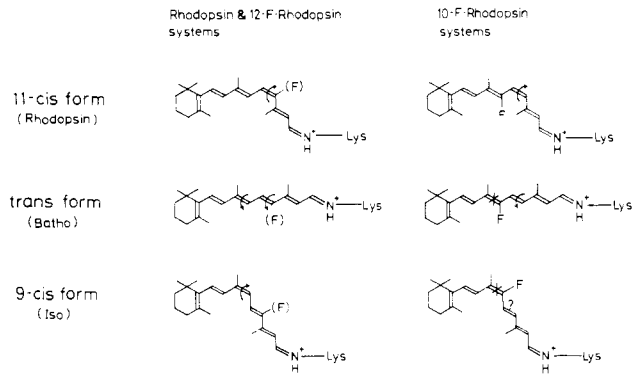

FIGURE 4: Possible photoisomerization models of rhodopsin, 12-F-rhodopsin, and 10-F-rhodopsin at liquid nitrogen temperature.

equal to those of the corresponding intermediates of cattle rhodopsin, while those of the 10-F-rhodopsin systems were slightly different; batho-10-F-rhodopsin was more stable than those of the cattle rhodopsin and 12-F-rhodopsin systems.

A photo-steady-state mixture produced by irradiation of 9-*cis*-10-F-rhodopsin at −191 °C was also warmed in a similar manner to those described above (data not shown). The bathochromic photoproduct formed at −191 °C was stable below −70 °C, and it was converted to 10-F-retinal and opsin above this temperature.

Discussion

The present results clearly demonstrate that the 10-F-rhodopsin system is uniquely different from the rhodopsin and 12-F-rhodopsin systems as reflected in its absorption property (Table I) and photochemical behavior (Figure 4). Though the photoisomerization at the 11,12-double bond is unaffected by the substitution of the fluorine atom for the hydrogen atom at C_{10} and C_{12} positions, only substitution at C_{10} (and not at C_{12}) inhibits the isomerization at the 9,10 double bond, making the photoisomerization of the all-trans form (and possibly the 9-cis) regiospecific at the 11,12 double bond. The regiospecific photoisomerizations of 10-F-rhodopsin and its photoproducts should be due to a specific interaction between the fluorine atom at C_{10} and the surrounding protein.

The extinction coefficient of batho-10-F-rhodopsin is much higher than that of the original 10-F-rhodopsin, while those of batho intermediates of rhodopsin and 12-F-rhodopsin are slightly higher than those of the original pigments. Furthermore, batho-10-F-rhodopsin is more stable than batho-rhodopsin and batho-12-F-rhodopsin. All these facts further suggest the existence of an unique specific chromophore–opsin interaction in the 10-F-rhodopsin system.

We may now consider the specific motion of the retinylidene chromophore in the retinal binding site during the process of the photoisomerization. It was formerly considered that the trimethylcyclohexenyl (β-ionone) ring region of the retinylidene chromophore relocated itself during the process of photoisomerization (Wald, 1968). However, since the discovery of the hydrophobic interaction between the opsin and the β-ionone portion of the chromophore (Matsumoto & Yoshizawa, 1975), a common view has been proposed that the isomerization would be caused by the rotation of the double bond system near the Schiff base region (Kawamura et al., 1979; Honig et al., 1979; Birge & Hubbard, 1980).

Figure 5 shows the schematic drawings of two possible ways of movement of the retinylidene chromophore caused by rotation at the 11,12 double bond that may take place during the isomerization from batho-10-F-rhodopsin to the 9-cis form; the processes a and b show the movements of the β-ionone ring region and the double bond system near the Schiff base region,

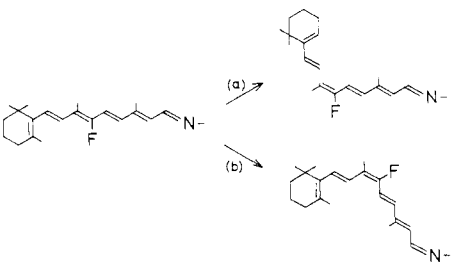

FIGURE 5: Schematic drawing of possible movements of the retinylidene chromophore in the retinal binding site of opsin during the isomerization of batho-10-F-rhodopsin. (a and b) Movements of the β-ionone ring region and the region near the Schiff base of the chromophore against the opsin, respectively. The fluorine atom at C_{10} displaces the position in (b) but not in (a) during the isomerization.

respectively. In process a the fluorine atom at C_{10} is fixed, while in process b it moves, resulting in a change of the interaction between the fluorine atom at C_{10} and the opsin. Thus, the fact that the isomerization of the 9,10 double bond was inhibited in batho-10-F-rhodopsin (and probably 9-*cis*-10-F-rhodopsin) suggests that the isomerization of rhodopsin to bathorhodopsin at the 11,12 double bond proceeds by movement of the half of the polyene chain containing the Schiff base, which may be accomodated by the movement of the butyl tether of the lysine residue.

Now the entity of the specific interaction between the fluorine atom at C_{10} and the opsin must be discussed. One of the candidates of the interaction may be a steric inhibition of rotation at the 9,10 double bond. The van der Waals radius of a fluorine atom and the bond distance between the fluorine and carbon atoms are both slightly larger than those in the case of a hydrogen atom [van der Waals radius; fluorine; 1.35 Å; hydrogen, 1.20 Å. Bond distance: F–C; 1.41 Å; H–C, 1.09 Å (Pauling, 1960)]. In the current version where the retinal binding site in opsin must be rather spacious for accomodating the rapid configurational and conformational changes during the primary process of rhodopsin and 9-*cis*-rhodopsin, this small increase in size caused by replacing a hydrogen atom with a fluorine atom in the chromophore seems unlikely to introduce a substantial steric interaction to the process of cis–trans isomerization.

Another possibility is an electrostatic interaction. A fluorine atom is highly electronegative, so that the C–F bond may be polarized by inducing a high electron density around the fluorine atom. This high electronegativity may interact in two possible ways: the first is an attractive interaction through a hydrogen bond with a neighboring acidic hydrogen such as a carboxyl, hydroxyl, sulfhydryl, or protonated amino group, and the second is a repulsive interaction with a neighboring group bearing an excessive electron density, e.g., a neighboring charged carboxylate ion, or electrophilic atoms such as an oxygen atom of carboxyl and hydroxyl and the sulfhydryl amino group.

Like bacteriorhodopsin, the higher order structure of rhodopsin is believed to be composed of seven α-helices each of which is penetrating the disk membrane (Dratz & Hargrave, 1983; Hargrave et al., 1984). The 11-*cis*-retinal binds to Lys^{296} of the seventh helix (helix 7) if the α-helices are numbered from the amino terminal. According to Matsumoto and Yoshizawa (1975), the β-ionone ring of the chromophore should interact specifically with the hydrophobic region of the opsin. The model of Hargrave (1984) indicates that helix 4 has no polarized amino acid residues. This highly hydrophobic region should be a possible location for binding with the β-ionone ring. Furthermore, the report by Honig et al. (1979) suggests the absence of an ion pair or a charged group near

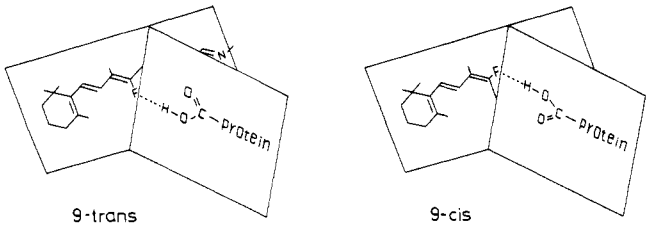

FIGURE 6: Postulated models of a hydrogen-bonding interaction between a carboxyl group and the fluorine atom in the 9-trans (left) and 9-cis (right) isomers.

the ring. Thus, helix 3, which contains three polarized amino acid residues, should not be located near the ring of the chromophore.

It is generally accepted that 11-*cis* retinal is bound to the lysine residue via a protonated Schiff base bond and the counterion is located near the Schiff base. If the protonated Schiff base forms a hydrogen bond with one of the three amino acid residues that have a carboxyl group (Dratz & Hargrave, 1983), the most plausible residue for the counterion may be Asp^{83} in helix 2 because of its proximity to the Schiff base. Glu^{122} or Glu^{134} in helix 3 is too far from the Schiff base for interaction. Whether or not other base units such as His^{211} in helix 5 and a tyrosine residue as recently shown to be the case in bacteriorhodopsin (Rothschild et al., 1986) can be a candidate of the counterion is not yet clear in rhodopsin. There is another positively charged group (Arg^{135}) in helix 3 that may form an ion pair with Glu^{134} because they are in close proximity to each other.

On the assumption of interaction of the β-ionone ring to helix 4 where no charged residue is present, the most probable amino acid residue that may interact with the fluorine atom at C_{10} may be Glu^{122}. Thus, helix 3, which contains Glu^{122}, should exist near the position of C_{10} (and not C_{12}) of the chromophore. There are two possible ways of interaction between Glu^{122} and the fluorine atom. If Glu^{122} is ionized, it would then interact repulsively with the electron-rich fluorine atom, thus suppressing the isomerization process,[2] especially when the polarization of the fluorine atom were accentuated in the excited state of the chromophore.

If Glu^{122} is not dissociated, the electron-rich fluorine atom may form a hydrogen bond with the carboxylic hydrogen atom of Glu^{122}. There is sufficient evidence in the literature to indicate the possible presence of such weak interactions between organofluorides and organic acids [see, e.g., Joesten and Schaad (1974), Carlson et al. (1972), and Jones and Watkinson (1964)]. The ΔH values of these interactions are of the same order in magnitude as the solvent-induced barrier for rotation (Loufty & Arnold, 1982), which is important in determining the direction of relaxation of planar excited polyenes (Franck–Codon structure) in solution photochemistry (Liu et al., 1983). Figure 6 shows the specific interaction of 9-*trans*-10-F-rhodopsin (batho-10-F-rhodopsin) (a) or 9-*cis*-10-F-rhodopsin (b) with a carboxyl group. It is clear that by way of either tautomerization or rotation of the carboxyl group only one such group is needed to interact with the fluorine atom on either side of the 9,10-double bond. This interaction may effectively block the isomerization of the C_9–C_{10} double bond.

[2] Birge et al. (1985) suggested from the two-photon spectroscopy and theoretical calculations that no negatively charged group except for the counterion exists near the chromophore of rhodopsin. However, they may not exclude the possibility of the existence of a negatively charged group that may interact with the fluorinated chromophore during the isomerization process from bathorhodopsin to 9-*cis*-rhodopsin.

We have no unambiguous experimental data yet to distinguish between these two possible ways of interactions just mentioned above (repulsive and hydrogen bond forming). Furthermore, at present it is not possible to pin point the amino acid residue responsible for the interaction with the fluorine atom at C_{10}. It is hoped that further experimental data such as vibrational spectroscopy on the C–F bond in these pigment analogues and related model compounds will provide key information to establish the nature of the protein–substrate interaction.

Photochemical reaction of 9-*cis*-10-F-rhodopsin is quite different from those of cattle 9-*cis*-rhodopsin and 9-*cis*-12-F-rhodopsin. On irradiation with 440-nm light at −191 °C, 9-*cis*-10-F-rhodopsin is converted to its bathochromic photoproduct, which was different from that produced from 10-F-rhodopsin. This bathochromic photoproduct is stable below −70 °C and converted to a mixture of 10-F-retinal and opsin at higher temperature. Therefore, it may be different in nature from the intermediate of rhodopsin. Since it is reasonable to assume that batho-10-F-rhodopsin produced from 10-F-rhodopsin has an all-trans geometry, the bathochromic photoproduct from 9-*cis*-10-F-rhodopsin must have a retinylidene chromophore different in configuration and/or conformation from it. The facts that this photoproduct has a low extinction coefficient and it was formed with a low quantum yield at room temperature suggest that the photoproduct may have a presently unknown geometry such as the 9,11-cis,cis, 9,13-cis,cis, or 13-cis form. Verification of its geometry will have to await completion of the chromophore extraction experiment of the irradiated sample of the 9-*cis*-10-F-rhodopsin at 191 °C.

REFERENCES

Balogh-Nair, V., & Nakanishi, K. (1982) in *New Comprehensive Biochemistry* (Tamm, Ch., Ed.) Vol. 3, pp 283–334, Elsevier Biomedical, Amsterdam.

Birge, R. R., & Hubbard, L. M. (1980) *J. Am. Chem. Soc. 102*, 2195–2205.

Birge, R. R., Murray, L. P., Pierce, B. M., Akita, H., Balogh-Nair, V., Findsen, L. A., & Nakanishi, K. (1985) *Proc. Natl. Acad. Sci. U.S.A. 82*, 4117–4121.

Carlson, G. L., Fateley, W. G., Manosha, A. J., & Bentley, F. F. (1972) *J. Phys. Chem. 76*, 1553–1557.

Dratz, E. A., & Hargrave, P. A. (1983) *Trends Biochem. Sci. (Pers. Ed.) 8*, 128–131.

Hargrave, P. A., McDowell, J. H., Feldman, R. J., Atkinson, P. H., Mohana, J. K., & Argos, P. (1984) *Vision Res. 24*, 1487–1499.

Hong, K., Knudsen, P. J., & Hubbell, W. L. (1982) *Methods Enzymol. 81*, 144–150.

Honig, B., Dinur, U., Nakanishi, K., Balogh-Nair, V., Gawinowicz, M. A., Arnaboldi, M., & Motto, M. G. (1979a) *J. Am. Chem. Soc. 101*, 7084–7086.

Honig, B., Ebrey, T., Callender, R. H., Dinur, U., & Ottolenghi, M. (1979b) *Proc. Natl. Acad. Sci. U.S.A. 76*, 2503–2507.

Joesten, M. D., & Schaad, L. J. (1974) *Hydrogen Bonding*, Dekker, New York.

Jones, D. A. K., & Watkinson, J. G. (1964) *J. Chem. Soc.*, 2366–2370.

Kakitani, H., Kakitani, T., Rodman, H., & Honig, B. (1985) *Photochem. Photobiol. 41*, 471–479.

Kawamura, S., Tokunaga, F., Yoshizawa, T., Sarai, A., & Kakitani, T. (1979) *Vision Res. 19*, 879–884.

Liu, R. S. H., Matsumoto, H., Asato, A. E., Denny, M., Shichida, Y., Yoshizawa, T., & Dahlquist, F. W. (1981) *J. Am. Chem. Soc. 103*, 7195–7201.

Liu, R. S. H., Asato, A. E., & Denny, M. (1983) *J. Am. Chem. Soc. 105*, 4829-4830.
Liu, R. S. H., Asato, A. E., Denny, M., & Mead, D. (1984) *J. Am. Chem. Soc. 106*, 8298-8300.
Liu, R. S. H., Crescitelli, F., Denny, M., Matsumoto, H., & Asato, A. E. (1986) *Biochemistry 25*, 7026-7030.
Loufty, R. O., & Arnold, B. A. (1982) *J. Phys. Chem. 86*, 4205-4211.
Maeda, A., Ogurusu, T., Shichida, Y., Tokunaga, F., & Yoshizawa, T. (1978) *FEBS Lett. 92*, 77-80.
Maeda, A., Shichida, Y., & Yoshizawa, T. (1979) *Biochemistry 18*, 1449-1453.
Matsumoto, H., & Yoshizawa, T. (1975) *Nature (London) 258*, 523-526.
Matsumoto, H., Horiuchi, K., & Yoshizawa, T. (1978) *Biochim. Biophys. Acta 501*, 257-268.
Matsumoto, H., Asato, A. E., Denny, M., Baretz, B., Yen, Y.-P., Tong, D., & Liu, R. S. H. (1980) *Biochemistry 19*, 4589-4594.
Ottolenghi, M. (1982) *Methods Enzymol. 88*, 470-491.
Pauling, L. (1960) *The Nature of the Chemical Bond*, Cornell University Press, New York.
Rothschild, K. J., Roepe, P., Ahl, P. L., Earnest, T. N., Bogomolni, R. A., Das Gupta, S. K., Mulliken, C. M., & Herzfeld, J. (1986) *Proc. Natl. Acad. Sci. U.S.A. 83*, 347-351.
Shichida, Y., Matuoka, S., & Yoshizawa, T. (1984) *Photobiochem. Photobiophys. 7*, 221-228.
Wald, G. (1968) *Nature (London) 219*, 800-807.
Yoshizawa, T. (1972) in *Handbook of Sensory Physiology* (Dartnall, H. J. A., Ed.) Vol. VII/1, pp 146-179, Springer-Verlag, Heidelberg.
Yoshizawa, T., & Wald, G. (1963) *Nature (London) 197*, 1279-1286.
Yoshizawa, T., & Shichida, Y. (1982) *Methods Enzymol. 81*, 333-354.
Yoshizawa, T., Shichida, Y., & Matuoka, S. (1984) *Vision Res. 24*, 1455-1463.

Microtubule Elongation and Guanosine 5′-Triphosphate Hydrolysis. Role of Guanine Nucleotides in Microtubule Dynamics

Marie-France Carlier,* Dominique Didry, and Dominique Pantaloni
Laboratoire d'Enzymologie, CNRS, 91190 Gif-sur-Yvette, France
Received December 29, 1986; Revised Manuscript Received March 11, 1987

ABSTRACT: The tubulin concentration dependence of the rates of microtubule elongation and accompanying GTP hydrolysis has been studied over a large range of tubulin concentration. GTP hydrolysis followed the elongation process closely at low tubulin concentration and became gradually uncoupled at higher concentrations, reaching a limiting rate of 35–40 s^{-1}. The kinetic parameters for microtubule growth were different at low and high tubulin concentrations. Elongation of microtubules has also been studied in solutions containing GDP and GTP in variable proportions. Only traces of GTP present in GDP were necessary to confer a high stability (low critical concentration) to microtubules. Pure GDP–tubulin was found unable to elongate microtubules in the absence of GTP but blocked microtubule ends with an equilibrium dissociation constant of 5–6 μM. These data were accounted for by a model within which, in the presence of GTP–tubulin at high concentration, microtubules grow at a fast rate with a large GTP cap; the GTP cap may be quite short in the region of the critical concentration; microtubule stability is linked to the strong interaction between GTP and GDP subunits at the elongating site; dimeric GDP–tubulin does not have the appropriate conformation to undergo reversible polymerization. These results are discussed with regard to the possible role of GDP and GTP and of GTP hydrolysis in microtubule dynamics.

It is well-known that GTP[1] hydrolysis accompanies microtubule assemby (Weisenberg et al., 1976) and that GTP is hydrolyzed by tubulin itself in this process (David-Pfeuty et al., 1977). The lack of tight temporal correlation between the time courses of tubulin spontaneous polymerization and accompanying hydrolysis of GTP indicated that these two reactions are not mechanistically coupled and GTP is hydrolyzed on microtubules following polymerization, which results in a core of subunits and stretches of GTP subunits at the ends of the growing microtubules [Carlier & Pantaloni, 1981; McNeal & Purich, 1978; for reviews see Carlier (1982) and Purich and Kristofferson (1984)]. These results together with the evidence for microtubule assembly in the presence of GMPPNP (Arai & Kaziro, 1976) showed that GTP hydrolysis was not necessary for tubulin polymerization; in contrast, GTP hydrolysis generates an unstable GDP polymer. The heterogeneity of microtubule subunits in GTP and GDP and the difference in their kinetic parameters were taken into account in a theoretical model for tubulin polymerization and GTP hydrolysis (Hill & Carlier, 1983) according to which the rate of microtubule elongation does not vary linearly vs. the concentration of dimeric tubulin, in contrast with the case of the reversible polymerization scheme described by Oosawa (1975); a sharp bend occurs at the critical concentration due to the rapid dissociation rate of GDP subunits from the polymer below the critical concentration. The theoretical predictions have been experimentally confirmed (Carlier et al., 1984a).

[1] Abbreviations: GTP, guanosine 5′-triphosphate; GDP, guanosine 5′-diphosphate; Ap_5A, P^1,P^5-bis(5′-adenosyl) pentaphosphate; EGTA, ethylene glycol bis(β-aminoethyl ether)-*N,N,N′,N′*-tetraacetic acid; MES, 2-(*N*-morpholino)ethanesulfonic acid; GMPPNP, guanosine 5′-(β,γ-imidotriphosphate); BSA, bovine serum albumin; HPLC, high-performance liquid chromatography.

0006-2960/87/0426-4428$01.50/0